Bound exciton luminescence in Te-doped SrS

Philip D. Rack, Jay S. Lewis, and Paul H. Holloway
Department of Materials Science and Engineering, University of Florida, Gainesville, Florida 32611-6400

Wounjhang Park, Brent K. Wagner, and Christopher J. Summers
Phosphor Technology Center of Excellence, Manufacturing Research Center, Georgia Institute of Technology, Atlanta, Georgia 30332-0560

(Received 11 February 1998; accepted for publication 7 July 1998)

This article describes the synthesis and characterization of SrS:Te powders which were found to have two high energy emission bands under photoluminescent excitation. To understand the radiative recombination mechanism, photoluminescence emission spectra were measured as a function of temperature. A simple configuration coordinate model was used to explain the emission band broadening and luminescence quenching that was observed with increasing temperature. Luminescence decay measurements were also performed, and the empirically determined transition rates were compared to theoretical calculations. Finally, SrS:Te ACTFEL devices were fabricated and tested under electroluminescence excitation. © *1998 American Institute of Physics.* [S0021-8979(98)08619-8]

I. INTRODUCTION

The idea of an isoelectronic trap was first introduced by Thomas *et al.*[1] in 1965 when they used this theory to describe the photoluminescence (PL) observed in GaP:N. They suggested that even though nitrogen had the same valence as phosphorus (isoelectronic), nitrogen acted as an electron trap in the GaP lattice. They reasoned that because nitrogen is significantly more electronegative than phosphorus, electrons are preferentially trapped at nitrogen sites. Subsequently, the N-electron complex has a net negative charge which sets up a short range Coulombic attraction for holes. Finally, when the hole is trapped, the electron and hole couple together and form an exciton. Because they are bound spatially in the nitrogen vicinity, these excitons are called bound excitons.

Since this model was suggested, the luminescent properties of other III–V, II–VI, and I–VII materials have been described by it. The focus of this article is on bound excitonic behavior in II–VI semiconductor materials, and in particular SrS:Te. For MS:Te (where M=Zn, Cd, or Sr) semiconductors, the bound exciton formation is similar to the GaP:N system except that the S host anion has a larger electronegativity than Te dopant. Because Te has a higher hole affinity than S, holes are trapped at Te sites forming a Te-hole complex. The Te-hole complex has a net positive charge which induces a Coulombic attraction for electrons. When the electron is trapped at this complex, a bound exciton is formed.

Of the MS:Te systems, CdS:Te and ZnS:Te have been studied the most. Aten *et al.*[2] first reported luminescence at 77 K in lightly doped CdS:Te (10^{18} cm^{-3}). They observed an emission band at 600 nm which was largely quenched at room temperature. Cuthbert and Thomas[3] later investigated both lightly and heavily doped CdS:Te (10^{18}–10^{20} cm^{-3}). They observed the 600 nm band and discovered another emission band at 730 nm in heavily doped samples. They attributed the 600 nm band to single Te_S sites (where Te_S represents a Te atom sitting substitutionally for a sulfur lattice site), and the 730 nm band to Te_S–Te_S pairs. They measured electron beam excited fluorescence spectra as a function of temperature and found that while the 600 nm band quenched severely above 175 K, the 730 nm band was stable up to room temperature. Later, Roessler[4] extensively studied the CdS:Te system, and from temperature dependent photoluminescent excitation and emission spectra he developed a configuration coordinate model to describe the CdS:Te bound exciton behavior. The 600 nm band zero-phonon line was estimated to be at 2.36 eV, and the phonon energy of the ground state and excited state was reported to be 21 and 14 meV, respectively. The thermal quenching of the luminescence was described, and it was found that the addition of shallow donors helped to increase the temperature where significant quenching of the luminescence occurred.

Isler and Strauss[5] were the first to report the optical properties of the ZnS:Te system. They showed two emission bands for the ZnS:Te with peak energies at 3.2 and 2.8 eV for the wurtzite phase and 3.1 and 2.7 eV for the zinc blende phase. They also attributed the high energy peaks to Te_S sites and the low energy peak to Te_S–Te_S sites. Fukushima and Shionoya[6] also studied the ZnS:Te system, and determined the phonon energies of the ground states and excited states, respectively. They also developed a configuration coordinate model to explain the bound exciton behavior in ZnS:Te, and used a similar model to describe the thermal quenching behavior they observed.

In this article, SrS:Te powders were synthesized and bound exciton emission from SrS:Te is reported. The luminescence properties of the SrS:Te powders are discussed in detail. In particular, the binding energy, the phonon energy, and the activation energy of nonradiative recombination for the bound excitons have been determined from temperature dependent PL emission spectra measurements. The luminescent decay times were also measured for both SrS:Te bound exciton emission bands, and finally SrS:Te thin film elec-

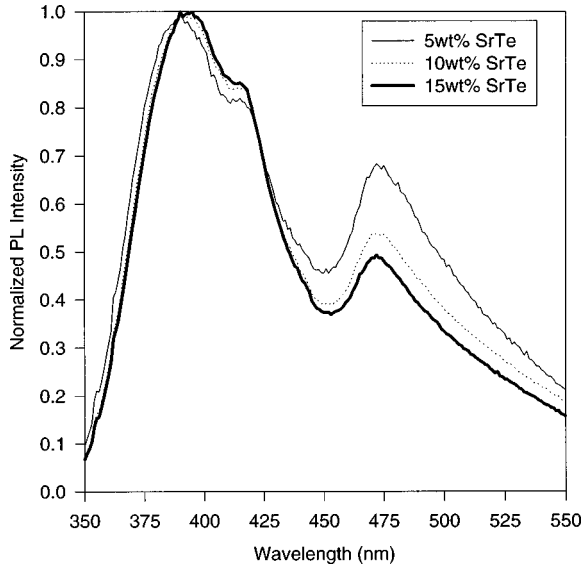

FIG. 1. Normalized PL emission spectra of SrS:Te powders.

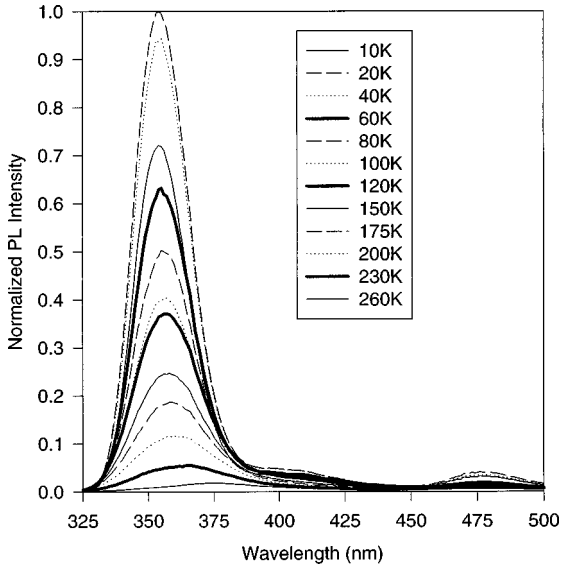

FIG. 2. Temperature dependent PL (275 nm excitation) emission spectra of 5 wt % SrTe powder (sample A).

troluminescent (TFEL) devices were fabricated to test this material as a possible phosphor material.

II. EXPERIMENTAL PROCEDURE

SrS:Te powders were synthesized by mixing different amounts of SrS and SrTe (SrTe=5, 10, and 15 wt %, SrS=100−SrTe wt %). The powder mixtures were then fired at 850 °C for 1 h in a nitrogen atmosphere, where they were cooled and then mixed with a mortar and pestle. The firing and mixing step was repeated six times for a total firing time of 6 h.

Temperature dependent photoluminescent measurements of the SrS:Te powders were taken with a 275 nm Ar ion laser. The 275 Ar ion laser had a 295 nm filter at the spectrometer to filter any reflected laser light, and the PL spectra were measured with a 1 nm resolution and the typical wavelength range was 300–500 nm. A liquid helium cold finger was used to cool the powder samples. In addition, temperature dependent PL spectra were also measured with a 325 nm He–Cd laser. The 325 nm He–Cd laser had a 350 nm filter at the spectrometer to filter any reflected laser light, and the spectra were also measured with a 1 nm resolution and a 350–550 nm wavelength range. X-ray diffraction scans were taken at room temperature for each powder using a Phillips APD 3720 diffractometer to characterize the composition and crystal structure.

To determine whether the SrS:Te thin films would emit under EL excitation, thin films were grown by molecular beam epitaxy (MBE) onto silicon and EL device substrates (glass/indium tin oxide/alumina-titania). To confirm whether Te was incorporated into the SrS, PL emission spectra of the SrS:Te thin films were measured using the Ar ion laser described above. Rutherford backscattering (RBS) was used to measure the Te concentration in one of the SrS:Te thin films and good agreement with the reported Te concentrations in other MS:Te systems was obtained.

III. RESULTS

The normalized room temperature PL data (325 nm excitation) for the SrS:Te powders are shown in Fig. 1. The emission peak maxima were positioned at about 400 nm, with a small shoulder at 475 nm. The temperature dependent PL emission spectra for sample A (initial SrTe concentration of 5 wt %), B (initial SrTe concentration of 10 wt %), and C (initial SrTe concentration of 15 wt %) are shown in Figs. 2, 3, and 4, respectively. 275 nm excitation was used for powders A and B, and 325 nm excitation was used for powder C.

The x-ray diffraction (XRD) scans for each powder contained peaks from both SrS and SrTe with the (200) and (220) peaks being dominant for both. High resolution scans of the SrS (200) and the SrTe (220) peaks were collected to determine if there were any detectable shifts in the XRD

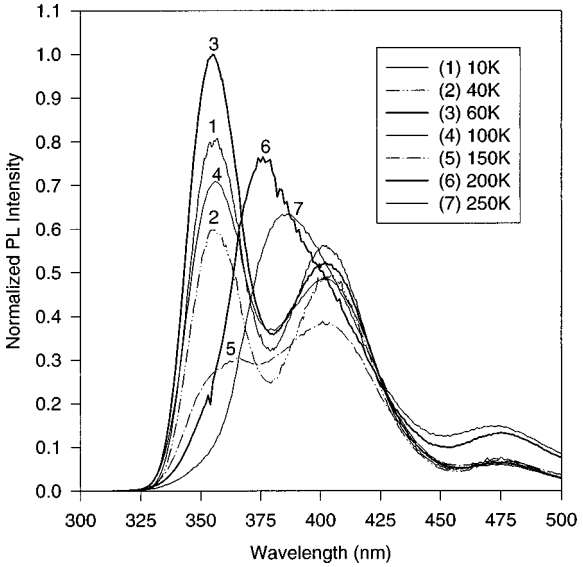

FIG. 3. Temperature dependent PL (275 nm excitation) emission spectra of 10 wt % SrTe powder (sample B).

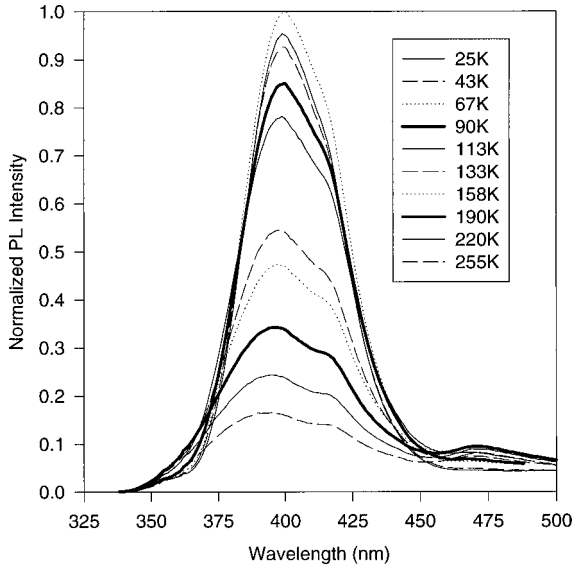

FIG. 4. Temperature dependent PL (325 nm excitation) emission spectra of 15 wt % SrTe powder (sample C).

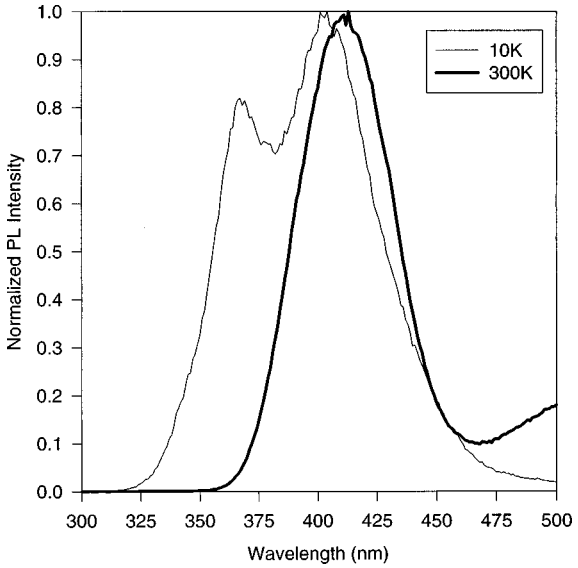

FIG. 5. 10 and 300 K PL emission spectra of MBE grown SrS:Te thin films.

peaks from the fired powder mixtures relative to pure SrS and SrTe. Peak shifts in the XRD data indicate changes in the lattice parameter, which can be correlated to the Te concentration assuming Vegard's Law. Table I summarizes the high resolution XRD results which demonstrate only very small shifts in the SrS and SrTe peaks. While the small peak shifts in the XRD patterns suggested a small amount of Te incorporation ($<10^{21}$ cm^{-3}), the peak shifts were not significant enough to precisely determine the Te concentration. Because not all of the SrTe went into solution with the SrS, at 850 °C there was either limited solubility for Te in SrS, or the Te diffusion in SrS was kinetically limited. The excess SrTe in the powders made it difficult to experimentally determine the Te concentration in the SrS:Te particles. The approximate Te concentrations will be discussed further in the discussion section.

The 10 and 300 K PL emission spectra for a SrS:Te thin film are shown in Fig. 5, which confirmed that Te was successfully incorporated in the SrS. The Te concentration for this film, as measured by RBS, was approximately 4.1 $\times 10^{19}$ cm^{-3}. Standard EL devices were fabricated and tested under EL excitation however, no luminescence was observed.

TABLE I. Summary of high resolution XRD results from SrS:Te powders.

Material	SrS (200) intensity	SrS (200) peak position	SrTe (220) intensity	SrTe (220) peak position	SrTe/SrS intensity (%)
SrS	···	29.686	···	···	···
SrTe 5%	40 080	29.6825	841	37.8075	2.09
SrTe 10%	48 620	29.6775	882	37.855	1.81
SrTe 15%	37 090	29.677	1221	37.86	3.29

IV. DISCUSSION

A. Te_S and Te_S–Te_S emission (sample B)

To determine the processes responsible for luminescence, initially temperature dependent PL measurements were collected from the 10 wt % SrTe powder (sample B). Figure 6 is a plot of the peak intensity versus temperature taken from Fig. 3. By comparing the temperature versus intensity plots in Fig. 6 to plots reported for ZnS:Te,[6] similar trends in the emission spectra were observed. The intensity fluctuations as a function of temperature were similar, and both of the high energy peaks quenched at approximately 200 K. Following the mechanism proposed for the ZnS:Te system, the two emission bands at 360 and 400 nm observed in the SrS:Te powders were attributed to bound exciton states created when Te substitutes isoelectronically on S lattice sites. Specifically, the 360 nm peak was assigned to excitons bound to single Te_S sites, whereas the 400 nm peak

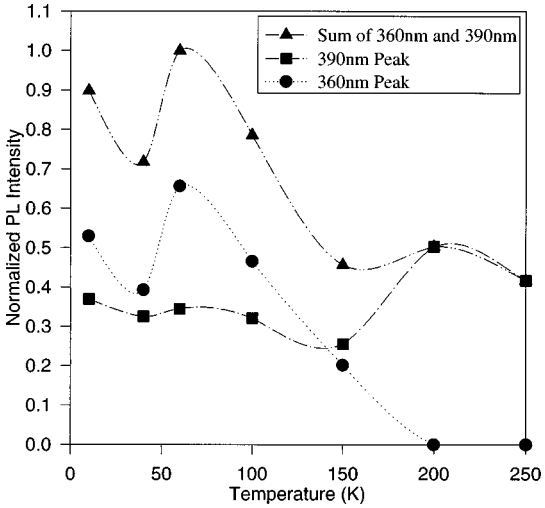

FIG. 6. PL intensity vs temperature for the 10 wt % SrTe powder (sample B).

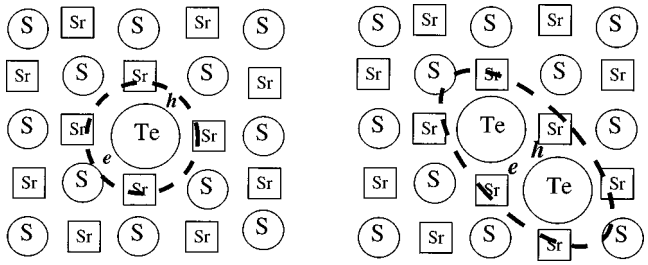

FIG. 7. Schematic diagram of Te_S and Te_S–Te_S sites in the SrS lattice.

was assigned to excitons bound to Te_S–Te_S pairs (see Fig. 7). The exact mechanism responsible for the 475 nm emission is not fully understood, however, a defect center is suspected. Because both emission bands exist at low temperatures, the Te concentration was estimated to be $\sim 5 \times 10^{19}$ cm^{-3}. At lower concentrations, the probability of forming Te_S–Te_S pairs is low, and at higher concentrations the probability of having Te_S singles is low.

As shown in Fig. 6, the PL intensity did not follow a systematic pattern as a function of temperature for the intermediate composition. This behavior is attributed to competing nonradiative recombination events which typically quench luminescence with increasing temperature, and energy transfer mechanisms which can increase luminescence as a function of temperature.[7] It is speculated that the single Te_S exciton emission band overlaps the excitation band for the Te_S–Te_S pairs, and similarly, the Te_S–Te_S pair exciton emission peak overlaps the defect center excitation spectra. When one emission band overlaps the excitation band of another, the emitted photon of the higher energy band can be reabsorbed by the lower energy band. In addition, the thermionic emission of bound electrons and holes can quench bands with lower binding energies and can recombine at deeper electron and hole traps. When energy transfer mechanisms occur between emission bands, it is difficult to distinguish between nonradiative recombination mechanisms and energy transfer mechanisms. Therefore, to characterize the Te_S and Te_S–Te_S excitons, the powders with lower (sample A) and higher (sample C) Te concentrations were analyzed.

B. Te_S emission (powder A)

To characterize the 360 nm emission from the single Te_S excitons, PL emission spectra (excited at 275 nm) for powder A were measured as a function of temperature. From the high resolution XRD data, this powder was believed to have a very low Te concentration because of the negligible SrS (200) peak shift. At sufficiently low Te concentrations, Te_S–Te_S pairs should not exist, therefore only the Te_S exciton band and the defect emission band should exist. Figure 2 confirmed that the single Te_S exciton band dominated the emission in this powder, and that the Te_S–Te_S band was virtually absent. Assuming similar bonding characteristics for Te in SrS versus ZnS or CdS and based on the concentrations necessary to eliminate the Te_S–Te_S band in ZnS:Te and CdS:Te, the Te concentration in the powder was estimated to be $\sim 5 \times 10^{18}$ cm^{-3}.

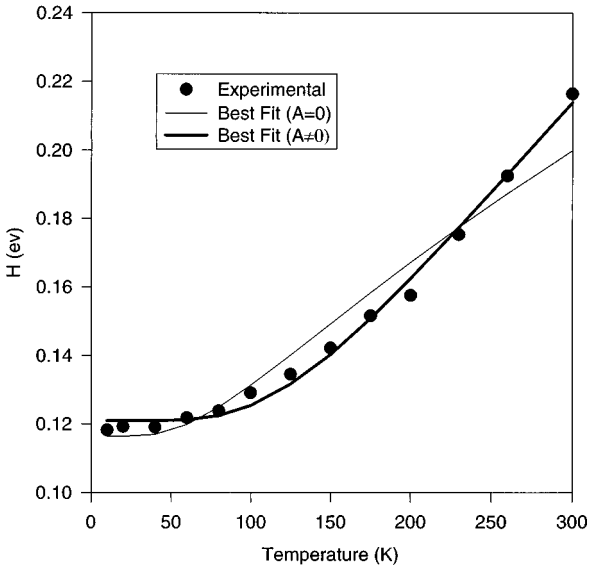

FIG. 8. The experimental and best fit of Eq. (2) ($A=0$ and $A\neq 0$) half width at half maximum vs temperature data for sample A (Te_S exciton).

1. Binding energy

By examining the 10 K emission spectra for this powder, the binding energy of the single Te_S bound exciton can be estimated. The bound exciton binding energy (BE_{ex}) is simply expressed by

$$BE_{ex} = BG - P(0), \tag{1}$$

where BG is the semiconductor band gap, and $P(0)$ is the zero-phonon line. Though the zero-phonon line was not observed even at 10 K, its energy position can be estimated as the high energy edge of the emission band. For the 360 nm band, the zero phonon line was approximately 3.76 eV (330 nm) and the SrS band gap is 4.32 eV. Therefore, the single Te_S bound exciton binding energy was approximately 0.56 eV.

2. Vibrational energy

Another useful parameter that can be determined from temperature dependent PL measurements is the phonon energy responsible for peak broadening. From the simple configuration coordinate model, the half width at half maximum (H) as a function of temperature is given by[4]

$$H(T)^2 = H(0)^2 \coth\left(\frac{h\omega}{2kT}\right) + A, \tag{2}$$

where $h\omega$ is the phonon energy, k is Boltzmann's constant, T is temperature, and A is a parameter used when the Frank–Condon approximation is not valid. Fitting Eq. (2) to half width at half maximum data from Fig. 2, and assuming the Frank–Condon principle applies ($A=0$), the phonon energy ($h\omega$) responsible for broadening the single Te_S exciton peak was determined to be 18.2 meV. Figure 8 compares the experimental H vs T data to the curve generated by the model.

To understand the physical significance of this phonon energy, it was compared to the phonon energies of the host SrS matrix. From reflectivity measurements, Kanekeo *et al.*[8]

determined that the longitudinal optical (LO) phonon energy and the transverse optical (TO) phonon energy of SrS were 35 and 23 meV, respectively. Assuming the Frank–Condon principle applies for the single Te_S bound exciton, the phonon energy responsible for the peak broadening (18.2 meV) matched well with the SrS TO phonon energy. While it was suspected that SrS would control the excited state vibrational energy for low Te concentration powders, the Frohlich interaction suggests that LO phonons couple better with excitons than do TO phonons.[9]

Because the calculated vibrational energy conflicted with the Frohlich interaction, the H vs T results were fit to Eq. (2) with $A \neq 0$ (i.e., Frank–Condon principle does not apply) as seen in Fig. 8. When the Frank–Condon principle was relaxed, the best fit of the H vs T data resulted in a phonon energy of 37.8 meV which was in good agreement with the LO phonon frequency of SrS (35 meV). From these results, it appears that for the Te_S bound exciton the vibrational energy is dominated by the SrS LO phonons, and for this transition the Frank–Condon principle does not apply.

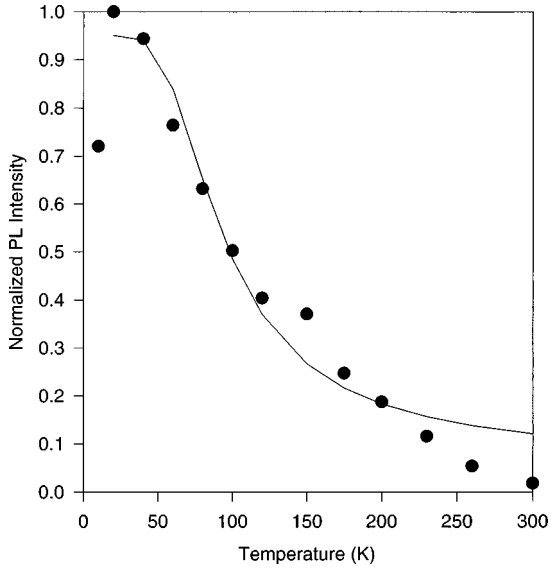

FIG. 9. Experimental and the best fit of Eq. (5) intensity vs temperature data for sample A (Te_S exciton).

3. Temperature quenching activation energy

From the temperature dependent emission spectra in Fig. 2 it is noticed that the 360 nm peak is significantly quenched with increasing temperature. To understand this quenching phenomenon, the following equations for the radiative efficiency as a function of temperature $\eta(T)$ were applied:[10]

$$\eta(T) = \frac{I}{I(0)} = \frac{W_R}{W_R + W_{\mathrm{NR}}}, \tag{3}$$

where I is intensity, and W_R and W_{NR} are the radiative and nonradiative recombination rates, respectively. W_{NR} is expressed by the temperature dependent expression

$$W_{\mathrm{NR}}(T) = W(0)\exp(-E/kT), \tag{4}$$

where $W(0)$ is of the order of the lattice vibrational frequency, E is an activation energy, k is Boltzmann's constant, and T is temperature. Combining Eqs. (3) and (4) results in the following expression of intensity (I) as a function of temperature:

$$I(T) = \frac{I(0)}{1 + A\ \exp\left(\dfrac{-E}{kT}\right)}, \tag{5}$$

where $A = W(0)/W_R$. According to these expressions, the nonradiative recombination rate increases with temperature while the radiative recombination rate is temperature insensitive. Subsequently, the radiative efficiency decreases as the temperature increases due to an increase in the nonradiative recombination rate.

Fitting Eq. (5) to the I vs T data from Fig. 2 results in an activation energy of 25.5 meV and an A value of 18.4. A plot of the experimental I vs T data compared to the theoretical model is shown in Fig. 9. The calculated activation energy was significantly lower than the binding energy (0.56 eV) of the single Te_S bound exciton, so the quenching mechanism was not attributed to thermalization of the bound exciton. Fukushima and Shionova[6] and Roessler[4] observed that the luminescence quenching activation energy was comparable to the bound exciton binding energy in ZnS:Te and CdS:Te, respectively. They postulated a two step mechanism in which the electron is released first and then the hole. Therefore, the thermal quenching activation energy they calculated was associated with the binding energy of the hole. For the SrS:Te system, this mechanism is not plausible because the bound exciton depth was too deep to be responsible for the experimentally determined activation energy.

The mechanism that could be responsible for the 25.5 meV activation energy is the thermal release of the electron from the bound exciton. The released electron could either be recaptured by the same Te_S site or a nearby Te_S site, or conversely it could be trapped by other defects resulting in the nonradiative return to the ground state. If the distance between nearest-neighbor Te_S sites was greater than the electron diffusion length, then the thermally released electron would likely recombine nonradiatively before it has a chance to be recaptured by another Te_S site. This process would effectively quench the bound exciton luminescence. If one assumed a perfectly uniform concentration of $5 \times 10^{18}\ \mathrm{cm}^{-3}$ Te atoms, the average distance between nearest-neighbor Te_S sites would be 5.8 nm. Because neither the free electron diffusion coefficient nor the mobility are known for SrS, accurate diffusion lengths for SrS could not be calculated. To estimate a diffusion length L for SrS, ZnS parameters were used (free electron diffusion coefficient $D = 2.92\ \mathrm{cm}^2/\mathrm{s}$ and minority carrier lifetime $\tau = 2.72 \times 10^{-14}$ s) to calculate the free electron diffusion length by using the equation $L = (D\tau)^{1/2}$. At 300 K, the electron diffusion length in ZnS is 3 nm which is significantly shorter than the Te_S nearest-neighbor distance (10 nm). Because the calculated diffusion length (3 nm) was smaller than the average distance between Te_S sites (5.8 nm), the thermalized electron will likely recombine nonradiatively before it reaches another Te_S site. While more sophisticated calculations are necessary to confirm this model, these rough calculations sug-

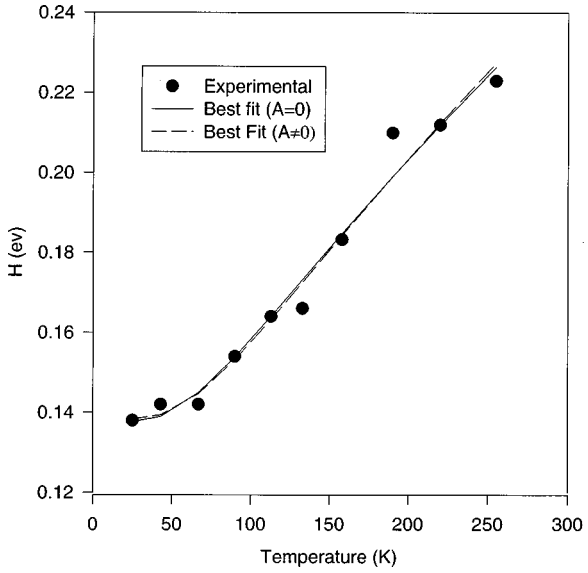

FIG. 10. Experimental and the best fit of Eq. (2) ($A=0$ and $A\neq 0$) half width at half maximum vs temperature data for sample C (Te_S–Te_S exciton).

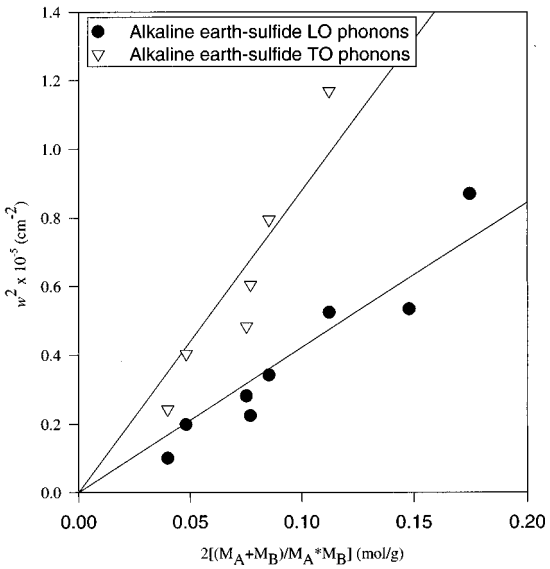

FIG. 11. Plot of ω^2 (LO and TO) vs $2(M_A+M_B)/M_AM_B$ for different alkaline-earth chalcogenide semiconductors. The slope of the linear regression is equal to the force constant used to determine the LO and TO phonon energies of SrTe.

gest that that the thermal release of electrons could be responsible for the observed temperature quenching of single Te_S bound excitons.

C. Te_S–Te_S emission

To characterize the 390 nm peak, attributed to Te_S–Te_S bound excitons, a 325 nm He–Cd laser was used to measure the temperature dependent emission spectra for the heavier doped (C) SrS:Te powder. Sample C was assumed to have a higher Te concentration because it had the highest initial SrTe concentration of 15 wt %. While the exact Te concentration was not experimentally determined, comparing the emission spectra of C to the ZnS:Te and CdS:Te data suggested a concentration of $\sim 10^{20}$ cm^{-3}. The 325 nm laser was used because the single Te_S exciton peak has a zero phonon line at approximately 330 nm, therefore, excitation of the single Te_S band at 325 nm is negligible. Consequently, energy transfer from the single Te_S band to the Te_S–Te_S band should be minimized, which would otherwise complicate the interpretation of the temperature dependent PL emission spectra.

1. Binding energy

By examining the 25 K emission spectra for this powder, the binding energy of the Te_S–Te_S bound exciton can also be approximated by using Eq. (1). Though the zero phonon line was not observed at 25 K, its energy position was approximated to be 3.44 eV (360 nm) and the SrS band gap is 4.32 eV. The single Te_S bound exciton binding energy is approximately 0.88 eV.

2. Vibrational energy

Using expression (2), the phonon energy responsible for broadening of the single Te_S–Te_S exciton peak was determined to be 17.0 meV when $A=0$, and 18.4 meV when $A\neq 0$. Figure 10 compares the experimental H vs T data taken from Fig. 4 to the points generated by the model. Again, when comparing this phonon energy to the LO (35 meV) and TO (23 meV) phonon energies of SrS, the experimentally determined phonon energy was significantly smaller. Because this emission peak comes from Te_S–Te_S pairs, it was suspected a local vibrational mode representative of the SrTe phonon energy could be dominating the vibration of the Te_S–Te_S pairs. While the LO and TO phonon energies of SrTe have not been reported, the SrTe phonon energies can be calculated using data from other alkaline-earth chalcogenide semiconductors. From the central force model, the TO and/or LO phonon frequency (at $k=0$) is given by[8]

$$\omega = \sqrt{2f\left(\frac{M_A+M_B}{M_AM_B}\right)} \tag{6}$$

where ω is the phonon frequency, f is the force constant, and M_A and M_B are the masses of the constituent ions in the semiconductor. The force constant (f) for the alkaline-earth chalcogenide semiconductors can be determined by taking the slope of the plot ω^2 vs $2(M_A+M_B)/M_AM_B$ (Fig. 11 where the phonon frequencies are taken from Ref. 8). From the linear regression of the data in Fig. 12, the TO and LO force constants for these materials were determined to be 422 914 and 879 757 mol/(g cm^2), respectively. Using the calculated force constants and the masses of Sr and Te, the TO and LO frequencies for SrTe were calculated to be 127.6 cm^{-1} (15.8 meV) and 184 cm^{-1} (22.8 meV), respectively.

Initially, the experimentally determined vibrational energy of 17.0 meV (when $A=0$) was also ascribed to the SrTe TO phonon energy, but because of the Frohlich interaction discussed previously, the $A=0$ restriction was lifted and the model was refit to the experimental data. For the condition $A\neq 0$, a phonon energy of 18.4 meV was determined which is in reasonable agreement with the calculated SrTe LO phonon energy (22.8 meV). This implies that the Te_S–Te_S pairs

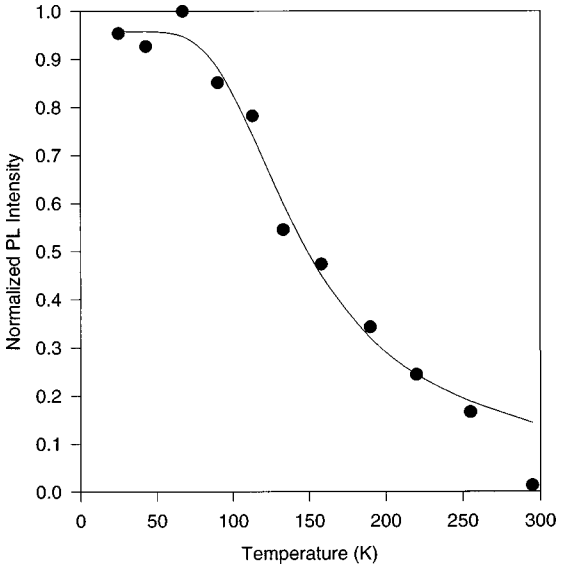

FIG. 12. Experimental and the best fit of Eq. (5) intensity vs temperature data for sample C (Te_S–Te_S exciton).

are vibrating at a different frequency than the SrS lattice, and the frequency is approximately that of the LO mode of SrTe. Because Eq. (2) satisfies the Frohlich interaction better when $A \neq 0$, this again implies that the Frank–Condon principle does not apply for the Te_S–Te_S bound exciton. Therefore, there is a significant difference between configuration of the ground state and excited state of the bound exciton.

3. Temperature quenching activation energy

The temperature quenching behavior of the Te_S–Te_S excitons, was again modeled by fitting Eq. (5) to the experimental data (Fig. 4) as shown in Fig. 12. An activation energy of 46.1 meV and an A value of 33.5 were determined. As for the lightly doped sample, the calculated activation energy was considerably lower than the binding energy (0.88 eV) of the Te_S–Te_S bound exciton, so the quenching mechanism was not attributed to thermalization of the bound exciton. The preferential thermalization of electrons is proposed as the quenching mechanism.

To determine whether the thermal activation of electrons could again be responsible for the observed temperature quenching, the distance between Te_S–Te_S pairs was again estimated. If a uniform distribution of 10^{20} pairs cm^{-3} is assumed, then the average distance between nearest-neighbor Te_S–Te_S pairs is about 2.1 nm. This is slightly smaller than the diffusion length calculated for ZnS above. From this rough calculation, it is difficult to conclude whether or not this mechanism could be responsible for the thermal quenching. Detailed simulations which consider the free electron trajectory, the temperature dependence of the SrS diffusion length, and the influence of the Te_S–Te_S Coulombic attraction are necessary to accurately model the mechanism and draw a conclusion.

D. Radiative recombination rate of Te_S and Te_S–Te_S bound excitons

Because the pre-exponential term (A) in Eq. (5) is inversely proportional to the radiative recombination rate, the ratio of $A(Te_S–Te_S)/A(Te_S)$ can be used to predict the relative radiative recombination rate of the Te_S and Te_S–Te_S bound excitons. If one assumes $W(0)$ is a constant then

$$A(Te_S-Te_S)/A(Te_S)=W_R(Te_S)/W_R(Te_S-Te_S)\simeq 1.8, \tag{7}$$

which suggests that the Te_S radiative recombination rate is approximately 1.8 times greater than that of the Te_S–Te_S bound exciton. To confirm whether this model accurately predicted the relative radiative recombination rates of the two bound excitons, this ratio was compared to the ratio of the decay lifetimes (τ) of the two emission bands. The decay constants (taken at $1/e$) were determined to be 0.6 (Te_S) and 0.9 μs (Te_S–Te_S), respectively. The ratio of these decay lifetimes indicate that the Te_S bound exciton radiative recombination rates is 1.5 times greater than the Te_S–Te_S bound excitons, which is in excellent agreement with the model predictions.

E. SrS:Te thin films

The 10 and 300 K PL spectra of the MBE grown SrS:Te film in Fig. 5 show that both the 360 nm peak (Te_S) and 400 nm peak (Te_S–Te_S) exists at 10 K and the 400 nm peak is dominant at 300 K. According to ZnS:Te literature data, the Te concentration should be between 5×10^{18} and 10^{20} cm^{-3} (i.e., $\sim5\times10^{19}$ cm^{-3}) since the two peak intensities were about equal at low temperature. From RBS measurements, the Te concentration was determined to be $\sim1.1\times10^{-3}$ at. % ($\sim4.1\times10^{19}$ cm^{-3}), which was consistent with the ZnS:Te concentrations. While the goal of investigating this phosphor material was to develop a bright blue EL phosphor, the SrS:Te did not emit under EL excitation. It is believed that the Te bound excitons are ionized by the high electric fields which is a process referred to as field quenching.

V. SUMMARY

SrS:Te phosphor powders were synthesized, and their luminescent properties were investigated. At low temperature, three high energy emission bands with peak energies of 360, 400, and 475 nm were identified. The 360 nm band was attributed to single Te_S bound excitons, the 400 nm band was attributed to Te_S–Te_S bound excitons, and the 475 nm band was tentatively attributed to a defect in the SrS lattice. By estimating the zero-phonon line of the bound exciton peaks, the binding energies for the Te_S and the Te_S–Te_S were calculated to be 0.56 and 0.88 eV, respectively. Using a simple configuration coordinate model, the Te_S phonon energy was calculated to be 37.8 meV. This value was in excellent agreement with the LO phonon energy of SrS, which suggests that the excited state is coupled with the host lattice. Similarly, the Te_S–Te_S phonon energy was calculated to be 18.4 meV which was in excellent agreement with the calculated LO phonon energy of SrTe.

The temperature quenching of the exciton emission was investigated, and the data were found to fit well with a common temperature quenching mechanism. The model used assumes that the radiative recombination rate is insensitive to temperature, however, the competing nonradiative recombination rate increases exponentially with increasing temperature. Nonradiative recombination activation energies of 25.5 and 46.1 meV were calculated for the Te_S and Te_S–Te_S excitons, respectively, which was interpreted to be the binding energy of the trapped electrons. The pre-exponential term in expression (5) that was used to model the temperature quenching behavior is inversely proportional to the radiative recombination rate. Thus, it was predicted that the Te_S bound exciton ($A=18.4$) should decay approximately 1.8 times faster than the Te_S–Te_S bound exciton ($A=33.5$). From the radiative decay lifetimes, the radiative recombination rate of Te_S bound exciton ($\tau=0.6\ \mu s$) was found to be approximately 1.5 times faster than the Te_S–Te_S bound exciton ($\tau=0.9\ \mu s$) which is in excellent agreement with the predicted value.

ACKNOWLEDGMENTS

This work was sponsored by the Phosphor Technology Center of Excellence (MDA972-93-1-0030 from DARPA). P.D.R. and P.H.H. would also like to acknowledge financial support from AFOSR (F 49620-96-1-0026).

[1] D. G. Thomas, J. J. Hopfield, and C. J. Frosch, Phys. Rev. Lett. **15**, 857 (1965).
[2] A. C. Aten, J. H. Haanstra, and H. D. Vries, Phillips Res. Rep. **20**, 395 (1965).
[3] J. D. Cuthbert and D. G. Thomas, J. Appl. Phys. **39**, 1573 (1968).
[4] D. M. Roessler, J. Appl. Phys. **11**, 4589 (1970).
[5] G. W. Isler and A. J. Strauss, J. Lumin. **3**, 1 (1970).
[6] T. Fukushima and S. Shionoya, Jpn. J. Appl. Phys. **12**, 549 (1973).
[7] G. Blasse and B. C. Grabmaier, *Luminescent Materials* (Springer, Berlin, 1994), p. 91.
[8] K. Kaneko, K. Morimoto, and T. Koda, J. Phys. Soc. Jpn. **51**, 2247 (1982).
[9] P. J. Dean and D. C. Herbert, in *Excitons*, edited by K. Cho (Springer, Berlin, 1979), p. 136.
[10] P. J. Dean and D. C. Herbert, in *Excitons*, edited by K. Cho (Springer, Berlin, 1979), p. 132.